ACSNANO

www.acsnano.org

ARTICLE

Effects of Surface Functional Groups on Electron Transfer at Liquid–Solid Interfacial Contact Electrification

Shiquan Lin,[Δ] Mingli Zheng,[Δ] Jianjun Luo, and Zhong Lin Wang*

Cite This: https://dx.doi.org/10.1021/acsnano.0c06075 Read Online

ACCESS | Metrics & More | Article Recommendations | Supporting Information

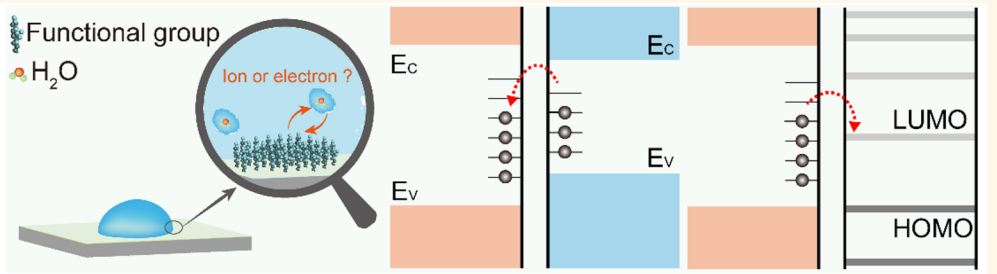

ABSTRACT: Contact electrification (CE) at interfaces is sensitive to the functional groups on the solid surface, but its mechanism is poorly understood, especially for the liquid–solid cases. A core controversy is the identity of the charge carriers (electrons or/and ions) in the CE between liquids and solids. Here, the CE between SiO_2 surfaces with different functional groups and different liquids, including DI water and organic solutions, is systematically studied, and the contribution of electron transfer is distinguished from that of ion transfer according to the charge decay behavior at surfaces at specific temperature, because electron release follows the thermionic emission theory. It is revealed that electron transfer plays an important role in the CE between liquids and functional group modified SiO_2. Moreover, the electron transfer between the DI water and the SiO_2 is found highly related to the electron affinity of the functional groups on the SiO_2 surfaces, while the electron transfer between organic solutions and the SiO_2 is independent of the functional groups, due to the limited ability of organic solutions to donate or gain electrons. An energy band model for the electron transfer between liquids and solids is further proposed, in which the effects of functional groups are considered. The discoveries in this work support the "two-step" model about the formation of an electric double-layer (Wang model), in which the electron transfer occurs first when the liquids contact the solids for the very first time.

KEYWORDS: *contact electrification, functional groups, electron transfer, thermionic emission, liquid–solid*

Contact electrification (CE) is a common phenomenon and can occur at almost any interface, including solid–solid interfaces and liquid–solid interfaces, and its mechanism remains poorly understood. Since that the CE may lead to discharge and explosion, it was always considered as a negative effect, until the invention of triboelectric nanogenerators (TENGs) to convert mechanical energy into electricity.[1−3] Owing to the invention of TENGs, the interest in CE is rekindled. Various methods were proposed to increase the surface charge transfer between two contact materials,[4,5] and the mechanism of CE was widely discussed.[6−10] It was demonstrated that the CE highly depends on the functional groups on the material surfaces,[11,12] and the output performance of both solid–solid TENGs[13−16] and liquid–solid TENGs[17−24] can be optimized by modifying functional groups on the solid surfaces. However, the mechanism of the chemical functional group contributions on the CE is still under debate, especially for the liquid–solid cases. A core controversy is the identity of the charge carriers in the CE (ion[25,26] or/and electron[27−29] transfer) between liquids and the functional group modified solid surfaces.

Received: July 20, 2020
Accepted: July 29, 2020
Published: July 29, 2020

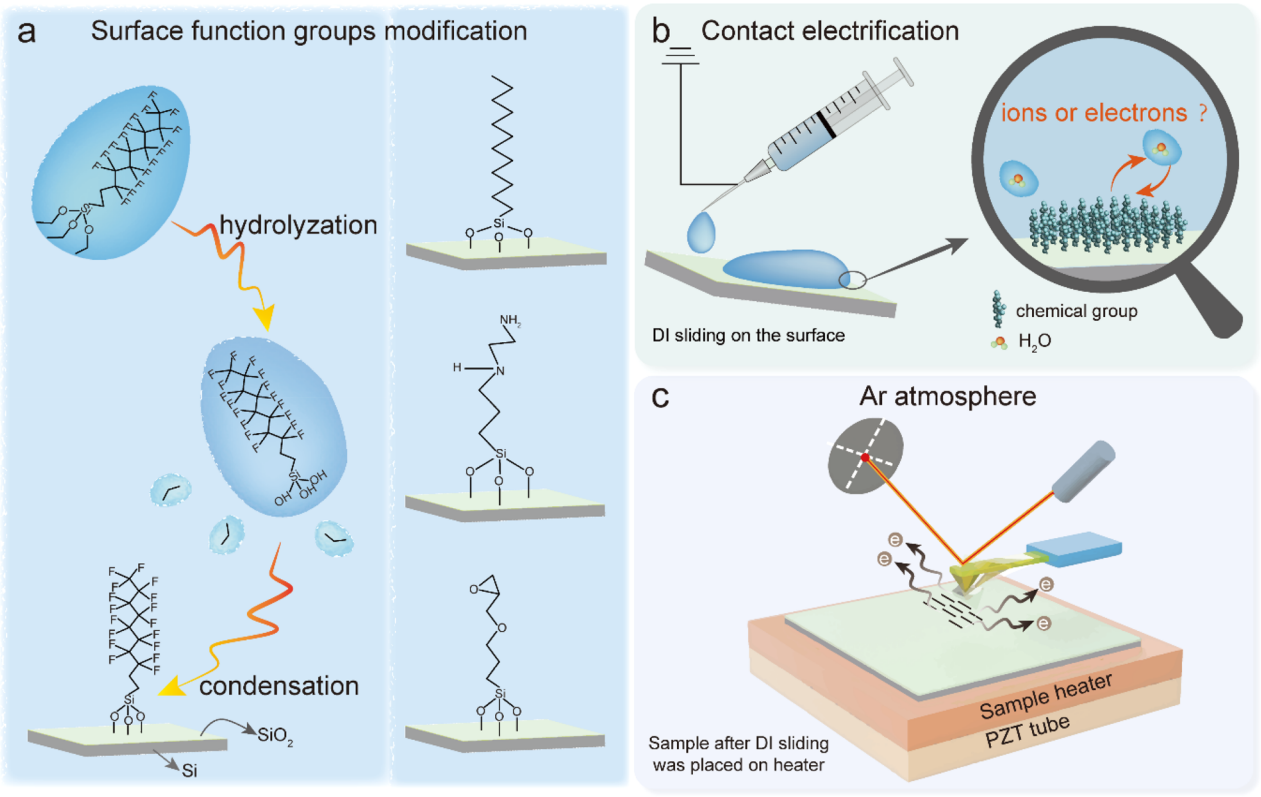

Figure 1. Schematic illustration of the chemical functional group modified surface. (a) Hydrolyzation of the silane coupling agents and the functional groups' self-assembly on the SiO_2 surfaces. (b) Contact electrification between liquid and the modified SiO_2 surface. (c) Setup of the AFM platform for the thermionic emission experiments and the measurements of the surface charge density.

From the point of view of ion transfer, the CE is caused by the movement of mobile counterions in the functional groups.[26] When a liquid (such as aqueous solution) is involved, the adsorption of the ions on the functional groups and the ionization or dissociation of the functional groups in the liquid should also be considered.[30,31] But an opposing opinion suggests that the CE between two different functional groups is highly dependent on the electron affinity of the elements in the groups,[11] so that the fluorine-containing groups (−F) always act as an electron acceptor and receive negative charges in the CE, while the amine groups ($-NH_2$) are always positively charged.[32] It was revealed that the electron transfer may be dominant in the CE between aqueous solutions and solids, as a consequence of the electron cloud overlap between the two atoms belonging to the aqueous solutions and solid surfaces.[33,34] Hence, the charge carriers in the CE between functional group modified solid surfaces and liquids have to be further identified. Fortunately, previous studies provide a method to quantify electron transfer and ion transfer between liquid and solid, in which the electrons are demonstrated to be easily emitted from the solid surfaces induced by thermionic emission.[35,36] For the ions on the solid surface, such as OH^- and H^+ on the SiO_2 surface, the energy threshold for removing the OH^- from the SiO_2 surface is about 8.5 eV,[37] and it is about 20 eV for removing the H^+.[38] Therefore, the ions (OH^- and H^+) are rather hard to be removed from the surfaces when the temperature is not too high.

In this paper, the CE between different liquids and the SiO_2 surfaces modified with different chemical functional groups is studied, and the surface charge density on SiO_2 surfaces is measured by using Kelvin probe force microscopy (KPFM).[39−41] The decay of CE charges on the modified SiO_2 surfaces at a temperature of 413 K is investigated. According to the thermionic emission theory, the contribution of electron transfer is distinguished from that of ion transfer in the CE. Particularly, we focused on the contributions of different functional groups to the contact electrification between liquid and solid. An energy band model for electron transfer is further proposed for the CE between liquids and functional group modified solid surfaces. It is suggested that the output performance of the triboelectric nanogenerators can be optimized by modifying different functional groups on solid surfaces. The findings in this work may have great implications in the applications based on the CE between liquid and solid.

RESULTS AND DISCUSSION

The liquid contact pair used in most of previous studies about liquid−solid CE is water, and ions are suspected as the charge carriers because of the existence of H^+ and OH^- in water. Here, besides the deionized water (DI water), the organic solutions (including dichloromethane, DCM, and cyclohexane, CYH) were used as the liquid contact pairs to avoid ion transfer and confirm electron transfer in liquid−solid CE. As shown in Figure 1a, the silane coupling agents with different functional groups were used to modify the SiO_2 surfaces, and four typical chemical functional groups (perfluorododecyl, oxypropyl, dodecyl, and aminopropyl) containing F, O, C, and N elements, respectively, were used in the experiments. The silane coupling agents were first dissolved in ethanol, and the SiO_2 samples were immersed in the solutions. In this process, the silane coupling agents will hydrolyze and self-assemble on

https://dx.doi.org/10.1021/acsnano.0c06075
ACS Nano XXXX, XXX, XXX−XXX

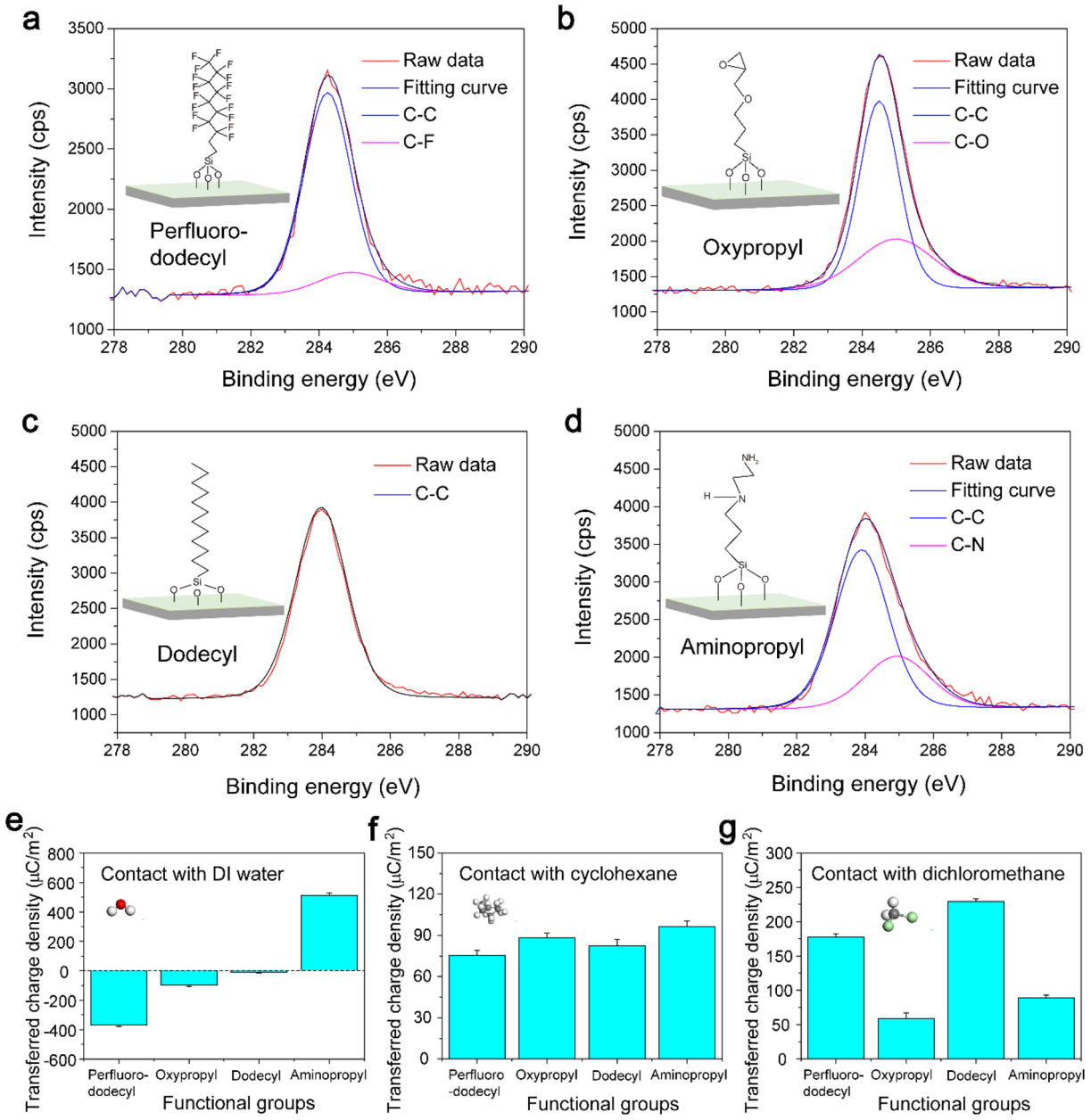

Figure 2. XPS characterizations of the modified SiO_2 surfaces and the contact electrification between the SiO_2 surfaces and different liquids. The XPS spectra of the SiO_2 surfaces modified with (a) perfluorododecyl, (b) oxypropyl, (c) dodecyl, and (d) aminopropyl. Transferred charge density on the different functional groups modified SiO_2 surfaces after contact with (e) DI water, (f) cyclohexane, and (g) dichloromethane.

the SiO_2 surfaces. The virgin modified SiO_2 surfaces were then contacted by the liquids, such as DI water, as shown in Figure 1b. The ions or electrons will transfer from the liquid to the solid surfaces in the contact. Then, the transferred charge density on the modified SiO_2 surfaces was measured by using KPFM, as shown in Figure 1c. The working principle of the KPFM was described elsewhere.[39] In order to distinguish electron transfer from ion transfer, the charged SiO_2 samples were heated by a sample heater to 413 K, and the decay of the surface charge density was recorded *in situ*. In our previous studies, the electrons were demonstrated to emit from solid surfaces at 413 K because of the thermionic emission, while the ions will stay on the surfaces at 413 K.[33]

The X-ray photoelectron spectra of the modified SiO_2 surfaces are shown in Figure 2a–d. The C–F, C–O, and C–N peaks can be extracted from the spectra of the perfluorododecyl-, oxypropyl-, and aminopropyl-modified SiO_2, respectively, and the F and N were detected on the perfluorododecyl- and aminopropyl-modified SiO_2 sample surfaces, respectively, as shown in Figure S1. For all of the SiO_2 samples, the C–C peaks were observed, but the elemental ratio of C to Si of the dodecyl-modified sample (0.39) is higher than that of the unmodified SiO_2 sample (0.27). (The carbon on the unmodified SiO_2 surface comes from the carbon-related contamination, which is hard to avoid once the SiO_2 sample is exposed to air.) These results suggest that all of the functional groups were successfully modified to the SiO_2 surfaces.

The transferred charge density on the modified SiO_2 surfaces after the contact with DI water is given in Figure 2e. The perfluorododecyl-, oxypropyl-, and dodecyl-modified

https://dx.doi.org/10.1021/acsnano.0c06075
ACS Nano XXXX, XXX, XXX–XXX

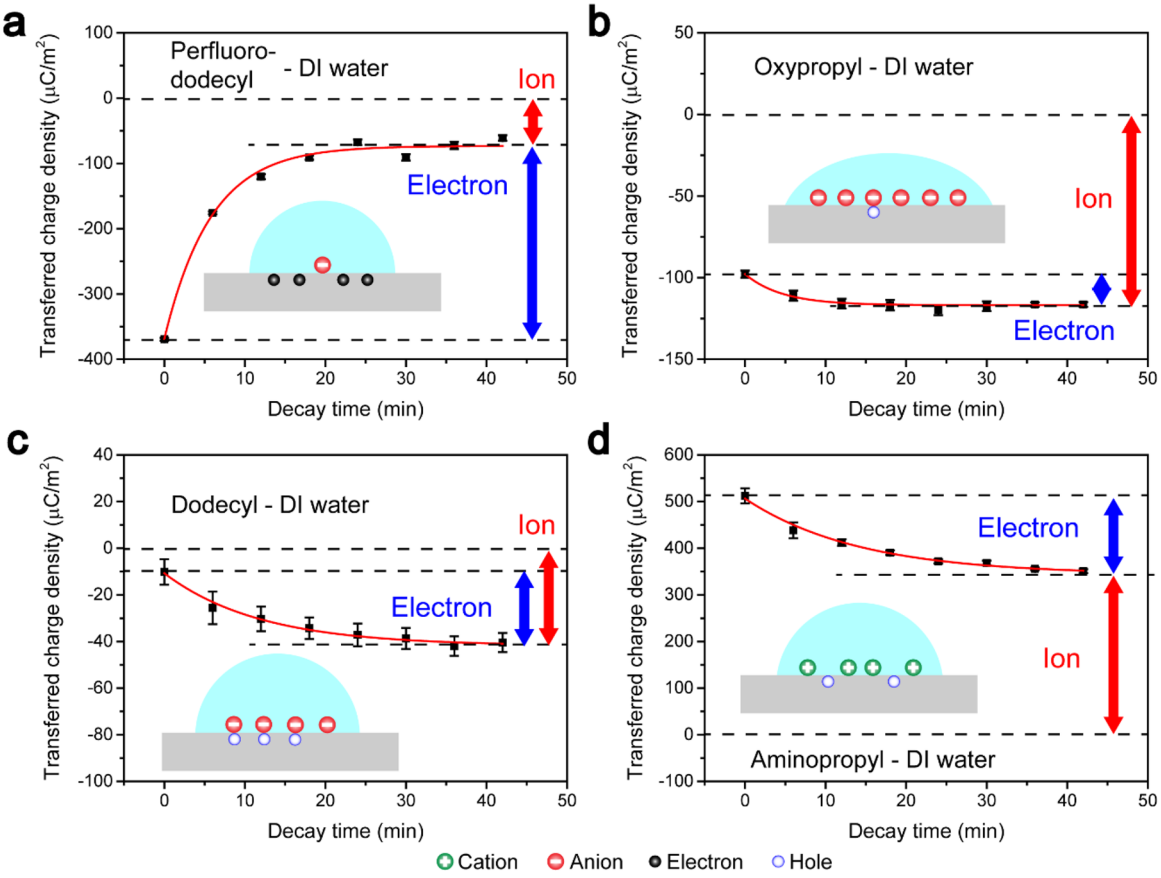

Figure 3. Temperature effect on the CE between DI water and the modified SiO_2 surfaces. Decay of the CE charges (induced by contacting with the DI water at room temperature) on the (a) perfluorododecyl-, (b) oxypropyl-, (c) dodecyl-, and (d) aminopropyl-modified SiO_2 surfaces at 413 K. Both physical adsorption (a, d) and chemical adsorption (b, c) of ions have been found at the interfaces.

SiO_2 samples received negative charge in the contact, while the aminopropyl-modified SiO_2 sample received positive charge. The transferred negative charge density on the perfluorododecyl-modified sample surface (about -370 $\mu C/m^2$) was much larger than that on the oxypropyl (about -110 $\mu C/m^2$) and dodecyl (-10 $\mu C/m^2$) modified sample surfaces. This is consistent with previous studies, in which the fluorine-containing groups are more likely to receive negative charge, while the amine groups are likely to be positively charged.[32] When the liquid contact pair was CYH, all the modified samples were positively charged, even the fluorine-containing sample, as shown in Figure 2f. It is noticed that there are no ions in the CYH, and ionization reaction is unlikely to occur between CYH and the functional group modified SiO_2 surfaces. Therefore, the charge carriers in the CE between CYH and modified SiO_2 samples seem to be electrons, since the adsorption of ions and ionization reaction are excluded. The electron transfer is mainly dependent on the CYH, instead of functional groups on the SiO_2 surfaces, because the amounts of transferred positive charges on different sample surfaces were almost the same (about 90 $\mu C/m^2$). Figure 2g gives the transferred charge density between modified SiO_2 samples and DCM. Similar to the CE between CYH and modified SiO_2 samples, all of the SiO_2 samples received positive charges in contact with DCM. The difference was that the amount of transferred charges on the SiO_2 surfaces varied from 60 $\mu C/m^2$ (oxypropyl-modified SiO_2) to 230 $\mu C/m^2$ (dodecyl-modified SiO_2). These results raise some questions. Does it mean that the CE between DI water and the modified SiO_2 only depends on the electron affinity of the elements in the functional groups, since that the fluorine-containing groups are negatively charged and amine groups are positively charged? Is there only electron transfer in the CE between the organic solutions and the modified SiO_2? The DCM and CYH are both organic solutions, why are they so different in the CE? In order to answer these questions, the contribution of electron transfer on the liquid–solid CE is distinguished from that of ion transfer according to the thermionic emission model, and the electron transfer and ion transfer are both discussed.

The decay of transferred charge density on the modified SiO_2 surfaces (generated by contacting with DI water) at 413 K is shown in Figure 3, and the decay of charge density on the unmodified SiO_2 surfaces was also performed as a control group, as shown in Figure S2. It is noticed that the charge density decayed exponentially for all of the samples, which follows the electron thermionic emission model in CE,[35,36] and some charges (about -70 $\mu C/m^2$ on the perfluorododecyl-modified SiO_2 surfaces) cannot be removed at 413 K, which can be called "sticky" charges. In previous studies, the removable charges are identified as electrons and the "sticky" charges are ions.[33] It can be seen that the unmodified SiO_2 samples received both electrons (-170 $\mu C/m^2$) and negative ions (-100 $\mu C/m^2$) in the CE (Figure S2). When the perfluorododecyl was added on the surfaces, the total negative transferred charge density increased from -270 $\mu C/m^2$ to -370 $\mu C/m^2$, as shown in Figure 3a. The electron transfer is found to dominate in the CE between the perfluorododecyl-modified samples and DI water (-300 $\mu C/m^2$), while the ion

https://dx.doi.org/10.1021/acsnano.0c06075
ACS Nano XXXX, XXX, XXX–XXX

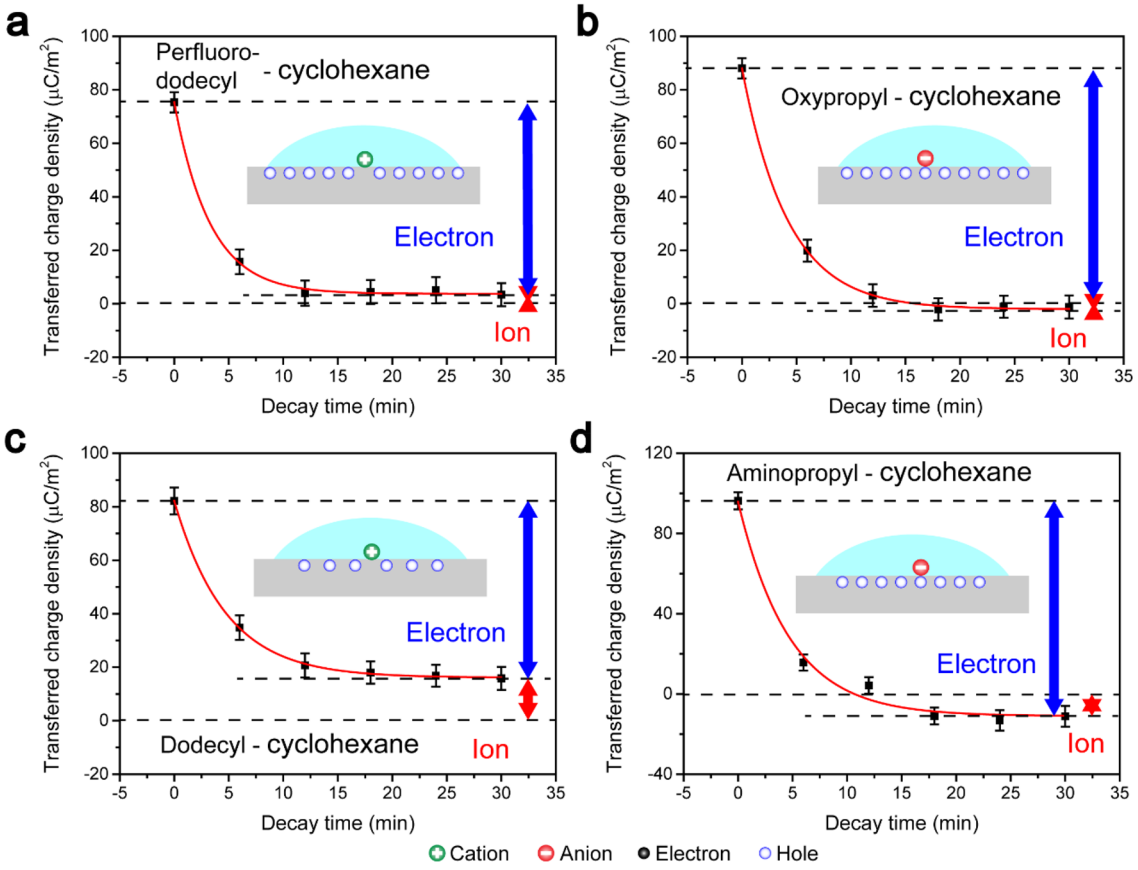

Figure 4. Temperature effect on the CE between the cyclohexane and the modified SiO_2 surfaces. The decay of the CE charges (induced by contacting with the cyclohexane at room temperature) on the (a) perfluorododecyl-, (b) oxypropyl-, (c) dodecyl-, and (d) aminopropyl-modified SiO_2 surfaces at 413 K. Both physical adsorption (a, c) and chemical adsorption (b, d) of ions have been found at the interfaces.

transfer was not significantly changed compared to that between the unmodified SiO_2 and DI water. For the oxypropyl (Figure 3b) and dodecyl (Figure 3c) modified SiO_2, the total negative charge density decreased to below -100 $\mu C/m^2$, and the polarity of electron transfer generated on the surfaces reversed to be positive (hole generated on the surfaces), while the ions generated on the surfaces remained negative. When the aminopropyl was added on the SiO_2 surface, the total transferred charges reversed to be positive, and both the holes and positive ions transferred from the DI water to the surface.

These results reveal that both electron transfer and ion transfer occur in the CE between the DI water and the modified SiO_2 (the ratios of ion transfer to electron transfer are shown in Figure S3), and the electron transfer is more sensitive to the surface functional groups than ion transfer. For the ion transfer, the aminopropyl tends to adsorb positive ions and makes the SiO_2 surface positively charged. But other functional groups in the experiments cannot significantly affect the ion transfer between the DI water and the SiO_2. For the electron transfer, perfluorododecyl acts as an electron acceptor and results in more electrons generated on the SiO_2 surfaces. Other groups act as electron donors and reverse the polarity of electron transfer. The electron affinity of the functional groups in the CE between DI water and the modified SiO_2 follows the order perfluorododecyl > oxypropyl ≈ dodecyl > aminopropyl. This is consistent with the CE between the Au-coated tip and modified SiO_2, in which the perfluorododecyl-modified SiO_2 received the most electrons and the transferred charges on other sample surfaces are more positive, as shown in Figure S4.

The decay of CE charges between modified SiO_2 and CYH is given in Figure 4. The decay curves were also exponential in this case, and almost all of the transferred charges were removed from modified SiO_2 surfaces at 413 K, which means that the CE between modified SiO_2 and CYH is electron transfer dominated. This is expected since that there are no ions in the CYH. Different from the CE between the modified SiO_2 and DI water, the electron transfer between the modified SiO_2 and the CYH was not significantly affected by the electron affinity of functional groups, and all of the transferred electron densities were about 90 $\mu C/m^2$. For the CE between different functional groups modified SiO_2 and the DCM (Figure 5), the electron transfer density also remained almost unchanged. The difference is that the positive ion transfer was observed when the modified functional group was perfluoro-dodecyl or dodecyl. The ion transfer may be caused by the DCM molecules being much more polar than the CYH molecules. The DCM molecules will form a hydrogen bond with water molecules in the atmosphere, while the number of water molecules adsorbed on the CYH surface will be very limited.[42,43] Hence, it is difficult to avoid the presence of water molecules in DCM and introducing ion transfer between the modified SiO_2 and the water molecules in DCM solutions.

The results show that electron transfer always exists in the liquid−solid CE and even plays a dominant role, whether the liquid is DI water or an organic solution. The electron transfer between DI water and solids is sensitive to the chemical functional groups on the solid surfaces, while the electron transfer between organic solutions and solids is not. Here, an

https://dx.doi.org/10.1021/acsnano.0c06075
ACS Nano XXXX, XXX, XXX−XXX

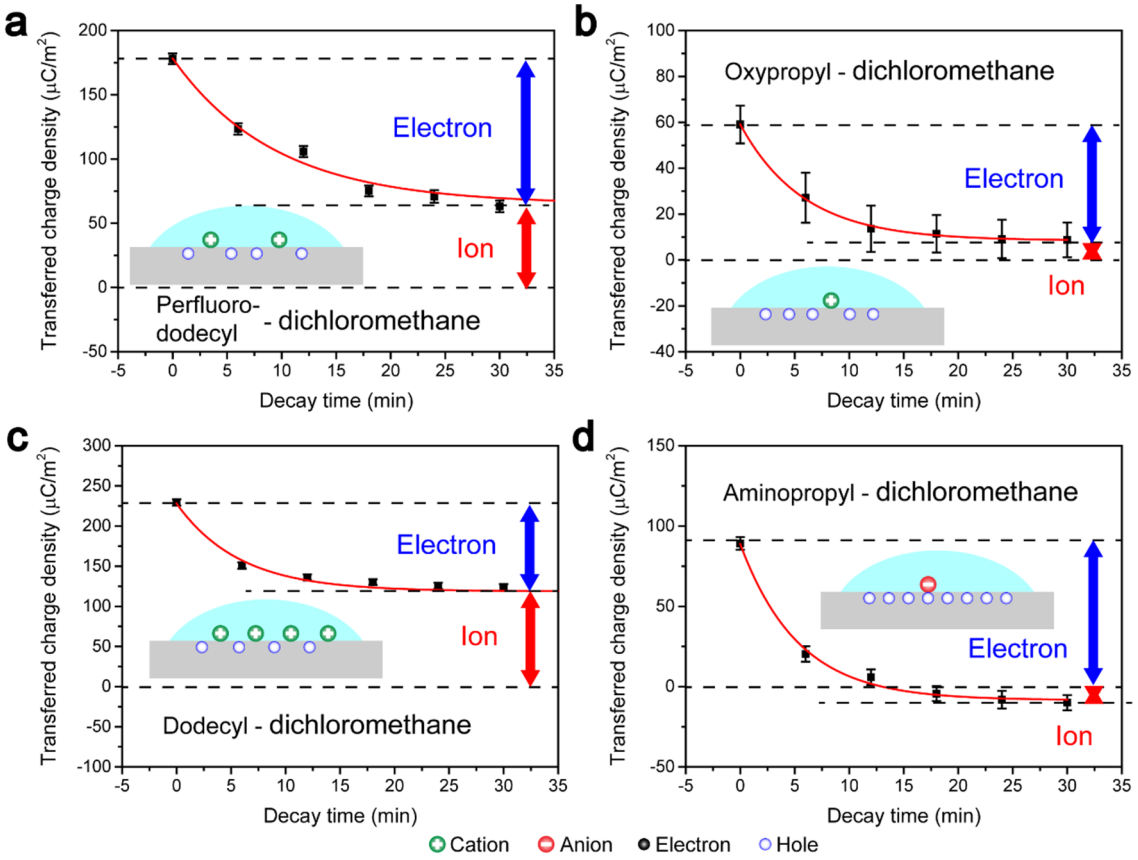

Figure 5. Temperature effect on the CE between the dichloromethane and the modified SiO_2 surfaces. The decay of the CE charges (induced by contacting with the dichloromethane at room temperature) on the (a) perfluorododecyl-, (b) oxypropyl-, (c) dodecyl-, and (d) aminopropyl-modified SiO_2 surfaces at 413 K. Both physical adsorption (a, b, c) and chemical adsorption (d) of ions have been found at the interfaces.

energy band model for the electron transfer between liquids and solids is proposed to explain the results in the experiments. Figure 6a gives the energy band diagram for the electron transfer between the unmodified SiO_2 and the DI water. (The energy scale in the diagram is based on previous studies,[44,45] in which the band gap of the SiO_2 is about 8.9 eV and the band gap of DI water is about 6.9 eV.) It is widely accepted that the surface states exist in the forbidden band of insulators, due to the surface defects and dangling bonds.[46−50] The electronic states of the liquid water was demonstrated to be similar to that of the amorphous semiconductors,[45] and the band gap of the liquid water is smaller than that of SiO_2.[51,52] In liquid water, the water molecules interact with each other by hydrogen bonding, resulting in many native impurities, such as clusters, H^+, and OH^-,[45] and the external impurities induced by the dissolution of oxygen and carbon dioxide also exist in liquid water, which may account for the very limited conductivity of DI water. The impurities may introduce additional electron energy levels in the forbidden band of the liquid water, which can be called "impurity states" of the liquid water, which are indicated in the figure. Hence, when the unmodified SiO_2 contacts the DI water, the electrons will transfer from the impurity states of the DI water to the surface states of the SiO_2 (the highest occupied energy level in the impurity states of DI water is higher than that in the surface states of SiO_2, since the SiO_2 received electrons in the experiments). The electron affinity has been demonstrated to affect electron transfer in contact electrification;[53,54] when the

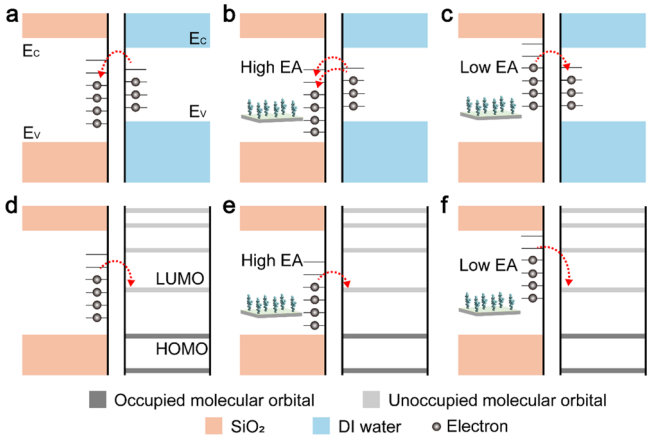

Figure 6. Energy band diagram for the CE between the modified SiO_2 surfaces with different liquids. (a) Electron transfer between the unmodified SiO_2 and DI water. The effects of (b) high electron affinity (EA) functional groups and (c) low electron affinity functional groups on the CE between SiO_2 and DI water. (d) Electron transfer between the unmodified SiO_2 and organic solutions. Effects of (b) high electron affinity functional groups and (c) low electron affinity functional groups on the CE between SiO_2 and organic solutions. (Ec is the bottom of the conductive band, Ev is the top of valence band, LUMO is the lowest unoccupied molecular orbital of the organic molecules, and HOMO is the highest occupied molecular orbital of the organic molecules.)

https://dx.doi.org/10.1021/acsnano.0c06075
ACS Nano XXXX, XXX, XXX−XXX

SiO_2 sample is modified by the high electron affinity chemical functional groups, such as perfluorododecyl, the highest occupied energy level in the surface states of SiO_2 will go down, because the high electron affinity groups will introduce unoccupied low-energy levels on the SiO_2 surface. In this case, more electrons will transfer from the impurity states of the DI water to the SiO_2 surface, as shown in Figure 6b. If the low electron affinity functional groups (such as aminopropyl) are modified on the SiO_2 surface, occupied high energy levels will be introduced on the surface and raise the highest occupied energy level in the surface states of SiO_2. The electrons will transfer from the SiO_2 surface to the DI water side, as shown in Figure 6c. It needs to be emphasized that when the DI water donates or receives electrons, the holes or electrons are shared by many water molecules in the liquid, instead of belonging to one or two water molecules, since the water molecules will be dissolved in a very short time if the electrons are donated.[55]

For the organic solutions (such as CYH and DCM), the molecules interact with each other by van der Waals force instead of hydrogen bonds, which means that the interaction between the organic molecules is much weaker than that between water molecules. Therefore, no native impurities or additional energy levels exist in the organic solutions, and the energy structure of the organic solutions can be described by the molecular orbital. As shown in Figure 6d, when the unmodified SiO_2 contacts the organic solutions, the electrons in the surface states of SiO_2 will transfer to the LUMO (lowest unoccupied molecular orbital) of the organic molecules, and the SiO_2 sample will be positively charged. It should be noticed that the molecular orbital is separated and there are at most two electrons in a molecular orbital. Hence, the ability of the organic solutions to donate or receive electrons is limited. Although the highest occupied energy level in the surface states of SiO_2 is much higher than the LUMO of the organic molecules, at most two electrons will transfer from the SiO_2 surface to the organic molecular. When the highest occupied energy level in the surface states of SiO_2 goes down due to the high electron affinity functional groups (Figure 6e), there are still two electrons that are going to transfer to organic solutions, as long as the highest occupied energy level of the SiO_2 is higher than the LUMO of the organic molecules. Similarly, the number of transferred electrons from the SiO_2 surface to the organic solution will not increase, although the highest occupied energy level of the SiO_2 goes up when the low electron affinity functional groups are modified on the SiO_2 surfaces. Hence, the density of electron transfer between the organic solutions and the SiO_2 samples was not sensitive to the functional groups on the SiO_2 surfaces in the experiments.

Different from the electron transfer, the ion transfer between the liquid and solid is not entirely dependent on the electron affinity of materials, since the holes (positive charges) and negative ions can be generated on the SiO_2 surface at the same time in the liquid–solid CE (Figure 3c). We believe that more data are required to reveal the mechanism of the ion transfer between liquid and solid.

It needs to be clarified that the charge decay experiments were performed after the liquid–solid CE, which means that the mechanism of the charge transfer at the liquid–solid interface is independent of the thermionic emission in the charge decay. The purpose of the charge decay experiments is to distinguish the electron transfer and ion transfer during liquid–solid CE. According to the thermionic emission experiments and the analysis, the questions raised in Figure 2 can be answered. The CE between the modified SiO_2 and DI water is the result of both electron transfer and ion transfer, in which the electron transfer depends on the electron affinity of the functional groups. For the CE between the organic solutions and the modified SiO_2, the electron transfer plays a dominant role, and the electron transfer cannot be significantly affected by the functional groups. The different transferred charge density in the CE between DCM and different functional-modified SiO_2 surfaces is caused by ion transfer, which is introduced by the water molecules in the DCM. These discoveries provide strong evidence for electron transfer in CE between liquids and solids, especially for that between organic solutions and solids. It implies that the electron transfer is ubiquitous and occurs as long as the electron clouds belonging to two atoms overlap.[56] The results in this study support the "two-step" model for the formation of an electric double-layer proposed by Wang,[57] in which the electron transfer is considered to be the first step to generate the charged solid surface, and the opposite ions in the liquid adsorb on the charged surface in the second step. Moreover, the traditional triboelectric series can be divided into two series based on this work: triboelectric electron series and triboelectric ion series. It is revealed that a material (oxypropyl- and dodecyl-modified SiO_2) can be located on the positive side in the electron series and negative side in the ion series at the same time. This finding provided a good idea to explain the triboelectric series.

CONCLUSIONS

In conclusion, different chemical functional groups were modified on the SiO_2 surfaces, and the CE between the modified SiO_2 surfaces and the liquids, including DI water and organic solutions, was investigated by KPFM. The contributions of electron transfer in the CE were distinguished from that of ion transfer by recording the decay curves of the transferred charge density at 413 K. The results suggest that there are both electron transfer and ion transfer in the CE between the modified SiO_2 and the DI water. It is found that the perfluorododecyl is likely to receive electrons and the aminopropyl tends to donate electrons, because of the different electron affinities of the groups. When the organic solutions, such as CYH and DCM, contact the modified SiO_2, the electron transfer plays a dominant role in the CE, since there are no ions in the organic solutions. The electron transfer between the organic solutions and the modified SiO_2 was independent of the functional groups on the SiO_2 surfaces. Based on the results, an energy band model for electron transfer is proposed to explain the CE between liquids and solids. The limited ability of the organic molecules to receive or donate electrons is considered responsible for the robustness of the electron transfer in the CE between the organic solutions and the modified SiO_2.

EXPERIMENTAL SECTION

Sample Preparations. The SiO_2 sample layer of 100 nm thickness was deposited on a heavily doped silicon wafer by thermal oxidation. The silane coupling agents, 1*H*,1*H*,2*H*,2*H*-perfluorodecyltriethoxysilane (vol. 0.7%), glycidyloxypropyl triethoxysilane (vol. 5%), and dodecyltrimethoxysilane (vol. 5%), were dissolved in absolute ethyl alcohol, and the SiO_2 samples were immersed in the solution for 4 h for the modification of perfluorododecyl, oxypropyl, and dodecyl, respectively. The unmodified SiO_2 samples are immersed in the absolute ethyl alcohol without silane coupling

https://dx.doi.org/10.1021/acsnano.0c06075
ACS Nano XXXX, XXX, XXX–XXX

agents for 4 h, as the control group. The dimethoxymethylsilyl aminopropyl (vol. 5%) was dissolved in 95% aqueous alcohol, and the SiO_2 samples were immersed in the solution for 8 min for the modification of aminopropyl. After the immersion, the samples were placed in a nitrogen atmosphere for 24 h and were heated to 433 K for 10 min. The water contact angles of the modified SiO_2 samples are given in Figure S5, and the DI water used in the experiments was produced by a deionizer (HHitech, China) with a resistivity of 18.2 MΩ·cm.

KPFM Measurements. The commercial AFM equipment Multimode 8 (Bruker, USA) with a heating module was used in the experiments. NSC 18 (MikroMash, USA; Au coated; tip radius: 25 nm; spring constant: 2.8 N/m) was used as the conductive tip. The heating and potential measurements were performed in an Ar atmosphere. In the KPFM measurement, the tapping amplitude was set to 300 mV, the scan size was 5 μm, and the lift height was 50 nm.

Experimental Details of the CE. Before the CE, the initial surface potential of the virgin sample surfaces was measured. Then, the liquids slid across the solid surface at room temperature, and the samples contacted by liquid were blown by N_2 gas, to make sure the liquid was all removed. Finally, the surface potential of the solid samples, which was changed by the transferred charge remaining on the surfaces, was measured again by using KPFM (in a dry argon atmosphere), and the average time for mounting the charged sample to the KPFM was about 1 min. The transferred charge density between the liquids and samples was calculated according to the change of the surface potential in CE.[33]

ASSOCIATED CONTENT

Supporting Information

The Supporting Information is available free of charge at https://pubs.acs.org/doi/10.1021/acsnano.0c06075.

Figures of the XPS characterization of the SiO_2 surfaces, temperature effect on the CE between the DI water and unmodified SiO_2, ratio of ion transfer to electron transfer in the contact electrification between liquid and modified SiO_2, CE between modified SiO_2 and Au-coated tip, water contact angle of the SiO_2 surfaces (PDF)

AUTHOR INFORMATION

Corresponding Author

Zhong Lin Wang − *Beijing Institute of Nanoenergy and Nanosystems, Chinese Academy of Sciences, Beijing 100083, People's Republic of China; School of Materials Science and Engineering, Georgia Institute of Technology, Atlanta, Georgia 30332-0245, United States;* orcid.org/0000-0002-5530-0380; Email: zlwang@gatech.edu

Authors

Shiquan Lin − *Beijing Institute of Nanoenergy and Nanosystems, Chinese Academy of Sciences, Beijing 100083, People's Republic of China; School of Nanoscience and Technology, University of Chinese Academy of Sciences, Beijing 100049, People's Republic of China*

Mingli Zheng − *Beijing Institute of Nanoenergy and Nanosystems, Chinese Academy of Sciences, Beijing 100083, People's Republic of China; School of Nanoscience and Technology, University of Chinese Academy of Sciences, Beijing 100049, People's Republic of China*

Jianjun Luo − *Beijing Institute of Nanoenergy and Nanosystems, Chinese Academy of Sciences, Beijing 100083, People's Republic of China; School of Nanoscience and Technology, University of Chinese Academy of Sciences, Beijing 100049, People's Republic of China*

Complete contact information is available at: https://pubs.acs.org/10.1021/acsnano.0c06075

Author Contributions

[Δ]These authors contributed equally: S. Lin and M. Zheng.

Notes

The authors declare no competing financial interest.

ACKNOWLEDGMENTS

This work is supported by the National Key R & D Project from Minister of Science and Technology (2016YFA0202704), National Natural Science Foundation of China (Grant Nos. 51605033, 51432005), and Beijing Municipal Science & Technology Commission (Z171100002017017, Y3993113DF).

REFERENCES

(1) Fan, F. R.; Tian, Z. Q.; Wang, Z. L. Flexible Triboelectric Generator! *Nano Energy* **2012**, *1*, 328−334.

(2) Zhu, G.; Bai, P.; Chen, J.; Jing, Q.; Wang, Z. L. Triboelectric Nanogenerators as a New Energy Technology: from Fundamentals, Devices, to Applications. *Nano Energy* **2015**, *14*, 126−138.

(3) Wang, Z. L. Triboelectric Nanogenerators as New Energy Technology for Self-Powered Systems and as Active Mechanical and Chemical Sensors. *ACS Nano* **2013**, *7*, 9533−9557.

(4) Ye, Q.; Wu, Y.; Qi, Y.; Shi, L.; Huang, S.; Zhang, L.; Li, M.; Li, W.; Zeng, X.; Wo, H.; Wang, X.; Dong, S.; Ramakrishna, S.; Luo, J. Effects of Liquid Metal Particles on Performance of Triboelectric Nanogenerator with Electrospun Polyacrylonitrile Fiber Films. *Nano Energy* **2019**, *61*, 381−388.

(5) Kim, D.; Lee, J.; You, I.; Kim, J.; Jeong, U. Adding a Stretchable Deep-Trap Interlayer for High-Performance Stretchable Triboelectric Nanogenerators. *Nano Energy* **2018**, *50*, 192−200.

(6) Lin, S.; Xu, L.; Zhu, L.; Chen, X.; Wang, Z. L. Electron Transfer in Nanoscale Contact Electrification: Photon Excitation Effect. *Adv. Mater.* **2019**, *31*, 1901418.

(7) Zhang, Y.; Shao, T. Contact Electrification Between Polymers and Steel. *J. Electrost.* **2013**, *71*, 862−866.

(8) Wu, J.; Wang, X.; Li, H.; Wang, F.; Hu, Y. First-Principles Investigations on the Contact Electrification Mechanism between Metal and Amorphous Polymers for Triboelectric Nanogenerators. *Nano Energy* **2019**, *63*, 103864.

(9) Persson, B.; Tartaglino, U.; Tosatti, E.; Ueba, H. Electronic Friction and Liquid-Flow-Induced Voltage in Nanotubes. *Phys. Rev. B: Condens. Matter Mater. Phys.* **2004**, *69*, 235410.

(10) Burgo, T.; Galembeck, F.; Pollack, G. Where is Water in the Triboelectric Series? *J. Electrost.* **2016**, *80*, 30−33.

(11) Lowell, J.; Brown, A. Contact Electrification of Chemically Modified Surfaces. *J. Electrost.* **1988**, *21*, 69−79.

(12) Horn, R.; Smith, D.; Grabbe, A. Contact Electrification Induced by Monolayer Modification of a Surface and Relation to Acid−Base Interactions. *Nature* **1993**, *366*, 442−443.

(13) Lin, Z.; Xie, Y.; Yang, Y.; Wang, S.; Zhu, G.; Wang, Z. L. Enhanced Triboelectric Nanogenerators and Triboelectric Nanosensor Using Chemically Modified TiO_2 Nanomaterials. *ACS Nano* **2013**, *7*, 4554−4560.

(14) Lee, J.; Cho, H.; Chun, J.; Kim, K.; Kim, S.; Ahn, C.; Kim, I.; Kim, J.; Kim, S.; Yang, C.; Baik, J. Robust Nanogenerators Based on Graft Copolymers via Control of Dielectrics for Remarkable Output Power Enhancement. *Sci. Adv.* **2017**, *3*, 1602902.

(15) Shin, S.; Bae, Y.; Moon, H.; Kim, J.; Choi, S.; Kim, Y.; Yoon, H.; Lee, M.; Nah, J. Formation of Triboelectric Series via Atomic-Level Surface Functionalization for Triboelectric Energy Harvesting. *ACS Nano* **2017**, *11*, 6131−6138.

(16) Chang, T.; Peng, Y.; Chen, C.; Chang, T.; Wu, J.; Hwang, J.; Gan, J.; Lin, Z. Protein-Based Contact Electrification and its Uses for

Mechanical Energy Harvesting and Humidity Detecting. *Nano Energy* **2016**, *21*, 238−246.
(17) Li, X.; Zhang, L.; Feng, Y.; Zhang, X.; Wang, D.; Zhou, F. Endocardial Pressure Sensors: Transcatheter Self-Powered Ultrasensitive Endocardial Pressure Sensor. *Adv. Funct. Mater.* **2019**, *29*, 1903587.
(18) Shahzad, A.; Wijewardhana, K. R.; Song, J. K. J. Contact Electrification Efficiency Dependence on Surface Energy at the Water-Solid Interface. *Appl. Phys. Lett.* **2018**, *113*, 023901.
(19) Choi, D.; Lee, S.; Park, S.; Cho, H.; Hwang, W.; Kim, D. Energy Harvesting Model of Moving Water Inside a Tubular System and its Application of a Stick-Type Compact Triboelectric Nanogenerator. *Nano Res.* **2015**, *8*, 2481−2491.
(20) Yin, J.; Zhang, Z.; Li, X.; Zhou, J.; Guo, W. Harvesting Energy from Water Flow over Graphene. *Nano Lett.* **2012**, *12*, 1736−1741.
(21) Okada, T.; Kalita, G.; Tanemura, M.; Yamashita, I.; Meyyappan, M.; Samukawa, S. Nitrogen Doping Effect on Flow-Induced Voltage Generation from Graphene-Water Interface. *Appl. Phys. Lett.* **2018**, *112*, 023902.
(22) Okada, T.; Kalita, G.; Tanemura, M.; Yamashita, I.; Meyyappan, M.; Samukawa, S. Role of Doped Nitrogen in Graphene for Flow-Induced Power Generation. *Adv. Eng. Mater.* **2018**, *20*, 1800387.
(23) Jeon, S.; Seol, M.; Kim, D.; Park, S.; Choi, Y. Self-Powered ion Concentration Sensor with Triboelectricity from Liquid-Solid Contact Electrification. *Adv. Electron. Mater.* **2016**, *2*, 160006.
(24) Kwak, S.; Lin, S.; Lee, J.; Ryu, H.; Kim, T.; Zhong, H.; Chen, H.; Kim, S. Triboelectrification-Induced Large Electric Power Generation from a Single Moving Droplet on Graphene/Polytetrafluoroethylene. *ACS Nano* **2016**, *10*, 7297−7302.
(25) Thomas, S.; Vella, S.; Dickey, M.; Kaufman, G.; Whitesides, G. Controlling the Kinetics of Contact Electrification with Patterned Surfaces. *J. Am. Chem. Soc.* **2009**, *131*, 8746−8747.
(26) MaCarty, L.; Winkleman, A.; Whitesides, G. Ionic Electrets: Electrostatic Charging of Surfaces by Transferring Mobile Ions upon Contact. *J. Am. Chem. Soc.* **2007**, *129*, 4075−4088.
(27) Li, S.; Nie, J.; Shi, Y.; Tao, X.; Wang, F.; Tian, J.; Lin, S.; Chen, X.; Wang, Z. L. Contributions of Different Functional Groups to Contact Electrification of Polymers. *Adv. Mater.* **2020**, *32*, 2001307.
(28) Byun, K.; Cho, Y.; Seol, M.; Kim, S.; Kim, S.; Shin, H.; Park, S.; Hwang, S. Control of Triboelectrification by Engineering Surface Dipole and Surface Electronic State. *ACS Appl. Mater. Interfaces* **2016**, *8*, 18519−18525.
(29) Tegenkamp, C.; Pfnur, H. Adsorbate Induced Contact Charging: Pure and OH^- Substituted Benzoic Acids Adsorbed on Wide Band Gap Insulators. *Phys. Chem. Chem. Phys.* **2002**, *4*, 2653−2659.
(30) Hiraga, Y.; Teramoto, Y.; Miyagawa, N.; Hoshino, K. Unexpected and Unusual Triboelectrification Behavior of Polymer Films Containing Carboxyl Group. *Langmuir* **2013**, *29*, 6903−6910.
(31) Israelachvili, J. *Intermolecular and Surface Forces 3*; Academic Press: CA, USA, 2011; Vol. *1*, p 291.
(32) Brennan, W.; Lowell, J.; Fellows, G.; Wilson, M. Contact Electrification and Surface Composition. *J. Phys. D: Appl. Phys.* **1995**, *28*, 2349−2355.
(33) Lin, S.; Xu, L.; Wang, A.; Wang, Z. L. Quantifying Electron-Transfer in Liquid-Solid Contact Electrification and the Formation of Electric Double-Layer. *Nat. Commun.* **2020**, *11*, 399.
(34) Nie, J.; Ren, Z.; Xu, L.; Lin, S.; Zhan, F.; Chen, X.; Wang, Z. L. Probing Contact-Electrification-Induced Electron and Ion Transfers at a Liquid−Solid Interface. *Adv. Mater.* **2020**, *32*, 1905696.
(35) Lin, S.; Xu, L.; Xu, C.; Chen, X.; Wang, A.; Zhang, B.; Lin, P.; Yang, Y.; Zhao, H.; Wang, Z. L. Electron Transfer in Nanoscale Contact Electrification: Effect of Temperature in the Metal−Dielectric Case. *Adv. Mater.* **2019**, *31*, 1808197.
(36) Xu, C.; Zi, Y.; Wang, A.; Zai, H.; Dai, Y.; He, X.; Wang, P.; Wang, Y.; Feng, P.; Li, D.; Wang, Z. L. On the Electron ransfer Mechanism in the Contact Electrification Effect. *Adv. Mater.* **2018**, *30*, 1706790.
(37) Burg, K.; Delahay, P. Photoelectron Emission Spectroscopy of Inorganic Anions in Aqueous Solution. *Chem. Phys. Lett.* **1981**, *78*, 287−290.
(38) Takakuwa, Y.; Niwano, M.; Nogawa, M.; Katakura, H.; Matsuyoshi, S.; Ishida, H. Photon-Stimulated Desorption of H^+ Ions from Oxidized Si(111) Surfaces. *Jpn. J. Appl. Phys.* **1989**, *28*, 2581−2586.
(39) Terris, B. D.; Stern, J. E.; Rugar, D.; Mamin, H. J. Contact Electrification Using Force Microscopy. *Phys. Rev. Lett.* **1989**, *63*, 2669.
(40) Lin, S.; Shao, T. Bipolar Charge Transfer Induced by Water: Experimental and First-Principles Studies. *Phys. Chem. Chem. Phys.* **2017**, *19*, 29418.
(41) Nonnenmachar, M.; O'Boyle, M. P.; Wickramasinghe, H. K. Kelvin Probe Force Microscopy. *Appl. Phys. Lett.* **1991**, *58*, 2921.
(42) Hore, D.; Walker, D.; MacKinnon, L.; Richmond, G. Molecular Structure of the Chloroform-Water and Dichloromethane-Water Interfaces. *J. Phys. Chem. C* **2007**, *111*, 8832−8842.
(43) Lopez, S.; Topalian, J.; Mitra, S.; Montague, D. Absorption and Desorption of Dichloromethane Vapor by Water Drops in Air. An Experimental Test of Scavenging Theory. *J. Atmos. Chem.* **1989**, *8*, 175−188.
(44) Jin, H.; Oh, S.; Kang, H.; Cho, M. Band Gap and Band Offsets for Ultrathin (HfO2) (SiO2) 1 − x Dielectric Films on Si(100). *Appl. Phys. Lett.* **2006**, *89*, 122901.
(45) Williams, F.; Varma, S.; Hillenius, S. Liquid Water as a Lone-Pair Amorphous Semiconductor. *J. Chem. Phys.* **1976**, *64*, 1549−1554.
(46) Lowell, J. The Electrification of Polymers by Metals. *J. Phys. D: Appl. Phys.* **1976**, *9*, 1571−1585.
(47) Hamilton, B.; Rose-Innes, A. Why Do Some Polymers Charge Positively? An Experimental Investigation. *J. Electrost.* **1981**, *10*, 121−127.
(48) Pong, W.; Brandt, D.; He, Z.; Imaino, W. Contact Charging of Insulating Polymers. *J. Appl. Phys.* **1985**, *58*, 896−901.
(49) Kwetkus, B.; Sattler, K. Analysis of Repeated-Contact Electrification Curves. *J. Phys. D: Appl. Phys.* **1992**, *25*, 1400−1407.
(50) Jean, M.; Hudlet, S.; Guthmann, C.; Berger, J. Local Triboelectricity on Oxide Surfaces. *Eur. Phys. J. B* **1999**, *12*, 471−477.
(51) Coe, J.; Earhart, A.; Cohen, M. Using Cluster Studies to Approach the Electronic Structure of Bulk Water: Reassessing the Vacuum Level, Conduction Band Edge, and Band Gap of Water. *J. Chem. Phys.* **1997**, *107*, 6023−6031.
(52) Shimkevich, A. The Lord Armstrong's Experiment in the View of Band Theory of Liquid Water. *Chem. Phys.* **2018**, *508*, 45−50.
(53) Lee, J.; Kim, K.; Choi, M.; Jeon, J.; Yoon, H.; Choi, J.; Lee, Y.; Lee, M.; Wie, J. Rational Molecular Design of Polymeric Materials Toward Efficient Triboelectric Energy Harvesting. *Nano Energy* **2019**, *66*, 104158.
(54) Kim, M.; Lee, Y.; Hur, Y.; Park, J.; Kim, J.; Lee, Y.; Ahn, C.; Song, S.; Ko, H. Molecular Structure Engineering of Dielectric Fluorinated Polymers for Enhanced Performances of Triboelectric Nanogenerators. *Nano Energy* **2018**, *53*, 37−45.
(55) Loh, Z.; Doumy, G.; Arnold, C.; Kjellsson, L.; Southworth, S.; Haddad, A.; Kumagai, Y.; Tu, M.; Ho, P.; Marck, A.; Schaller, R.; Yusof, M.; Simon, M.; Welsch, R.; Inhester, L.; Khalili, K.; Nanda, K.; Krylov, A.; Moeller, S.; Coslovich, G.; et al. Observation of the Fastest Chemical Processes in the Radiolysis of Water. *Science* **2020**, *367*, 179−182.
(56) Lin, S.; Xu, C.; Xu, L.; Wang, Z. L. The Overlapped Electron-Cloud Model for Electron Transfer in Contact Electrification. *Adv. Funct. Mater.* **2020**, *30*, 1909724.
(57) Wang, Z. L.; Wang, A. C. On the Origin of Contact-Electrification. *Mater. Today* **2019**, *30*, 34.

https://dx.doi.org/10.1021/acsnano.0c06075
ACS Nano XXXX, XXX, XXX−XXX